Science of the Total Environment 639 (2018) 476–484

Contents lists available at ScienceDirect

Science of the Total Environment

journal homepage: www.elsevier.com/locate/scitotenv

Potential land use adjustment for future climate change adaptation in revegetated regions

Shouzhang Peng [a], Zhi Li [b,*]

[a] State Key Laboratory of Soil Erosion and Dryland Farming on the Loess Plateau, Northwest A&F University, Yangling 712100, China
[b] College of Natural Resources and Environment, Northwest A&F University, Yangling 712100, China

HIGHLIGHTS

- We evaluated the sustainability of current vegetation in China's Loess Plateau.
- Future potential natural vegetation was predicted by a dynamic vegetation model.
- Only 25.3%–55% of forests in 2010 can be kept over 2071–2100 in this region.
- Adjustment of land use pattern is essential to adapt to climate change.

GRAPHICAL ABSTRACT

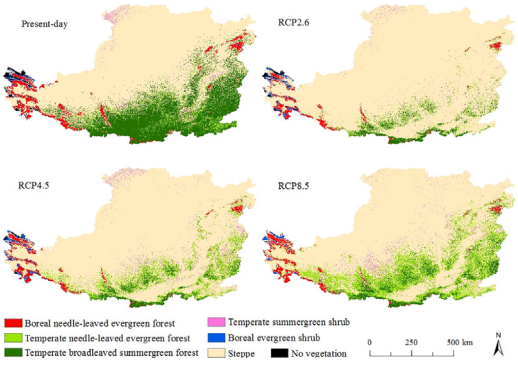

ARTICLE INFO

Article history:
Received 20 February 2018
Received in revised form 18 April 2018
Accepted 15 May 2018
Available online 26 May 2018

Editor: D. Barcelo

Keywords:
Climate change
Land use adjustment
LPJ-GUESS
Potential natural vegetation
Revegetated regions

ABSTRACT

To adapt to future climate change, appropriate land use patterns are desired. Potential natural vegetation (PNV) emphasizing the dominant role of climate can provide a useful baseline to guide the potential land use adjustment. This work is particularly important for the revegetated regions with intensive human perturbation. However, it has received little attention. This study chose China's Loess Plateau, a typical revegetated region, as an example study area to generate the PNV patterns with high spatial resolution over 2071–2100 with a process-based dynamic vegetation model (LPJ-GUESS), and further investigated the potential land use adjustment through comparing the simulated and observed land use patterns. Compared with 1981–2010, the projected PNV over 2071–2100 would have less forest and more steppe because of drier climate. Subsequently, 25.3–55.0% of the observed forests and 79.3–91.9% of the observed grasslands in 2010 can be kept over 2071–2100, and the rest of the existing forested area and grassland were expected to be more suitable for steppes and forests, respectively. To meet the request of China's Grain for Green Project, 60.9–84.8% of the existing steep farmland could be converted to grassland and the other for forest. Our results highlight the importance in adjusting the existing vegetation pattern to adapt to climate change. The research approach is extendable and provides a framework to evaluate the sustainability of the existing land use pattern under future climate.

1. Introduction

Land use change, due to climate change and human activities, can greatly alter the environment including climate (Pielke, 2005), hydrology (Chen et al., 2015), soil carbon stocks (Deng et al., 2014), and

* Corresponding author.
E-mail address: lizhibox@nwafu.edu.cn (Z. Li).

https://doi.org/10.1016/j.scitotenv.2018.05.194
0048-9697/

primary productivity (Albani et al., 2006), and further brings adverse effects if those changes exceed the environmental carrying capacity of an area. Thus, the consistency of those changes with potential natural vegetation (PNV), dominating by climate and ignoring the impacts of human activities (Chiarucci et al., 2010; Zerbe, 1998), has always been paid great attention. The prerequisite of these studies is to determine the PNV and the extent that the observed pattern overlaps with the NPV, which provides fundamental information to effectively regulate the human activities-induced land use change.

Further, the global warming and increasing carbon dioxide (CO_2) concentration has resulted in large-scale vegetation change across the planet according to those evaluations with the ecosystem models and climate change scenarios on regional and global scales (Hickler et al., 2012; Piao et al., 2006; Piao et al., 2013; Wolf et al., 2008), and it will continue to influence the structure, function, and distribution of vegetation ecosystems in future (Dai et al., 2016; Friend et al., 2014). Can the existing vegetation adapt to future climate change and how will the current land use patterns evolve? Evaluation of this aspect can provide important information for land use management.

This kind of evaluation is especially important for those regions with revegetation programs such as the Grain for Green Project in China (GGP) (Chen et al., 2015), the Bonn Challenge in Germany (Verdone and Seidl, 2017), and the Initiative 20 × 20 launched by Latin American and Caribbean countries (Crouzeilles et al., 2016). With intensive human perturbation, the vegetation in these regions has been experiencing a rapid change. For example, vegetation cover in the key area of GGP has almost doubled between 1999 and 2013 according to satellite imagery (Chen et al., 2015), and the Bonn Challenge launched in 2011 plans to restore 350 million ha of degraded forest landscapes by 2030 (Verdone and Seidl, 2017). These programs are implemented according to some criteria; for example, the GGP in China requires farmlands with slopes >25° to be returned to grasslands or forests. With intensive perturbation in a short period, the ability of the land use pattern to adapt to future climate change should be further investigated.

China's Loess Plateau (CLP), located in the middle reach of the Yellow River (Fig. 1), is one of the most severely eroded areas in the world (Zhao et al., 2013). It was, therefore, chosen as the pilot region for the GGP in 1999 (Li et al., 2017). Subsequently, the change speeds of the normalized difference vegetation index over 2000–2015 were ten times of those in 1982–1999, among which human activities account for 55% of the change (Li et al., 2017). The GGP has effectively controlled soil erosion, and erosion levels have returned to historic values (Wang et al., 2016a). Despite this success, the revegetation program is approaching its water resource limits on CLP (Feng et al., 2016). Chen et al. (2015) argued that the revegetated area should be maintained, but not expanded further as originally planned. With substantial land use change and subsequent environmental changes, CLP has become an ideal area to investigate land use change and its environmental effects.

In this study, we used LPJ-GUESS (Smith et al., 2001; Smith et al., 2014), a process-based dynamic vegetation model, to simulate high-resolution PNV for the current time period and a future time period. We then compared the land use pattern from the PNV simulation with the land use pattern observed on CLP to investigate whether the current human-induced land use pattern is consistent with the future PNV and present information for land use adjustment under future climate.

2. Materials and methods

2.1. Study area

CLP has an area of 6.2×10^5 km^2. With an arid to sub-humid climate, the mean annual precipitation ranges from 96.1 to 1469.5 mm, and the mean annual temperature has a range of −8.9 to 14.7 °C (1960–2000) (Chinese National Ecosystem Research Network, 2017). The annual mean precipitation and temperature decrease from the southeast to the northwest. Compared with 1981–2010, the annual mean precipitation and temperature would increase during 2071–2100 (Peng et al., 2018). However, the change will vary with the intensity of radiative forcing, i.e. Representative Concentration Pathway (RCP). Different greenhouse gas concentration trajectories predict different changes in precipitation and temperature (Fig. 2): a 6% increase in precipitation and a 1.5 °C increase in temperature under RCP2.6, 12% and 2.3 °C under RCP4.5, and 22% and 4.3 °C under RCP8.5.

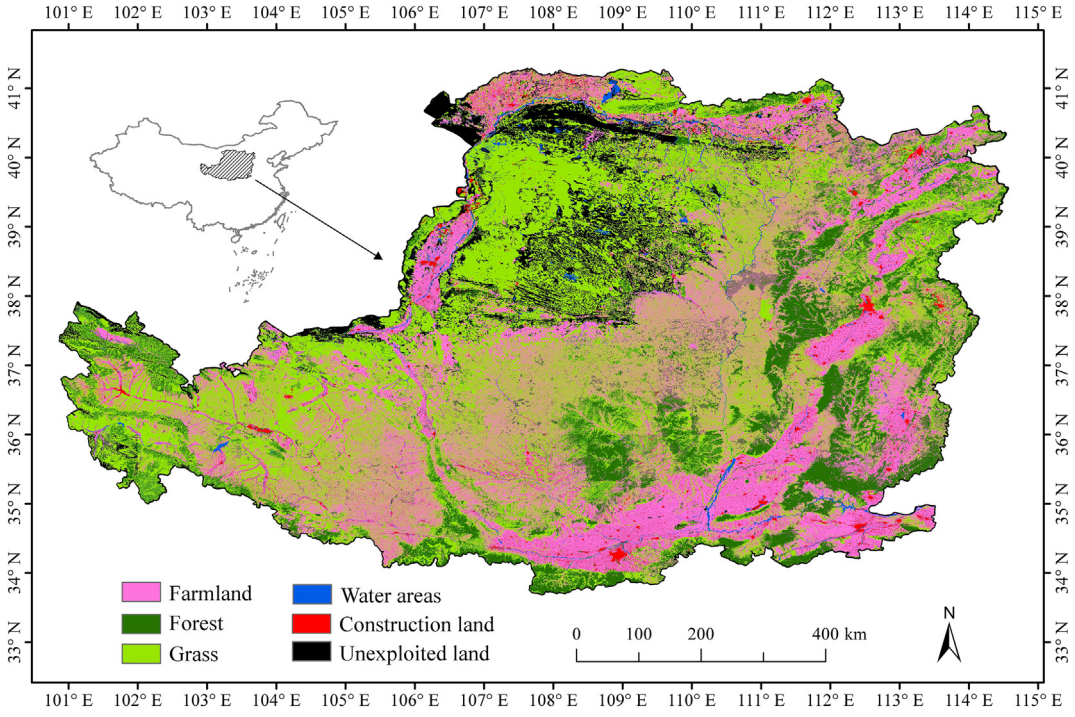

Fig. 1. Location of China's Loess Plateau and its land use in 2010 (Li et al., 2016).

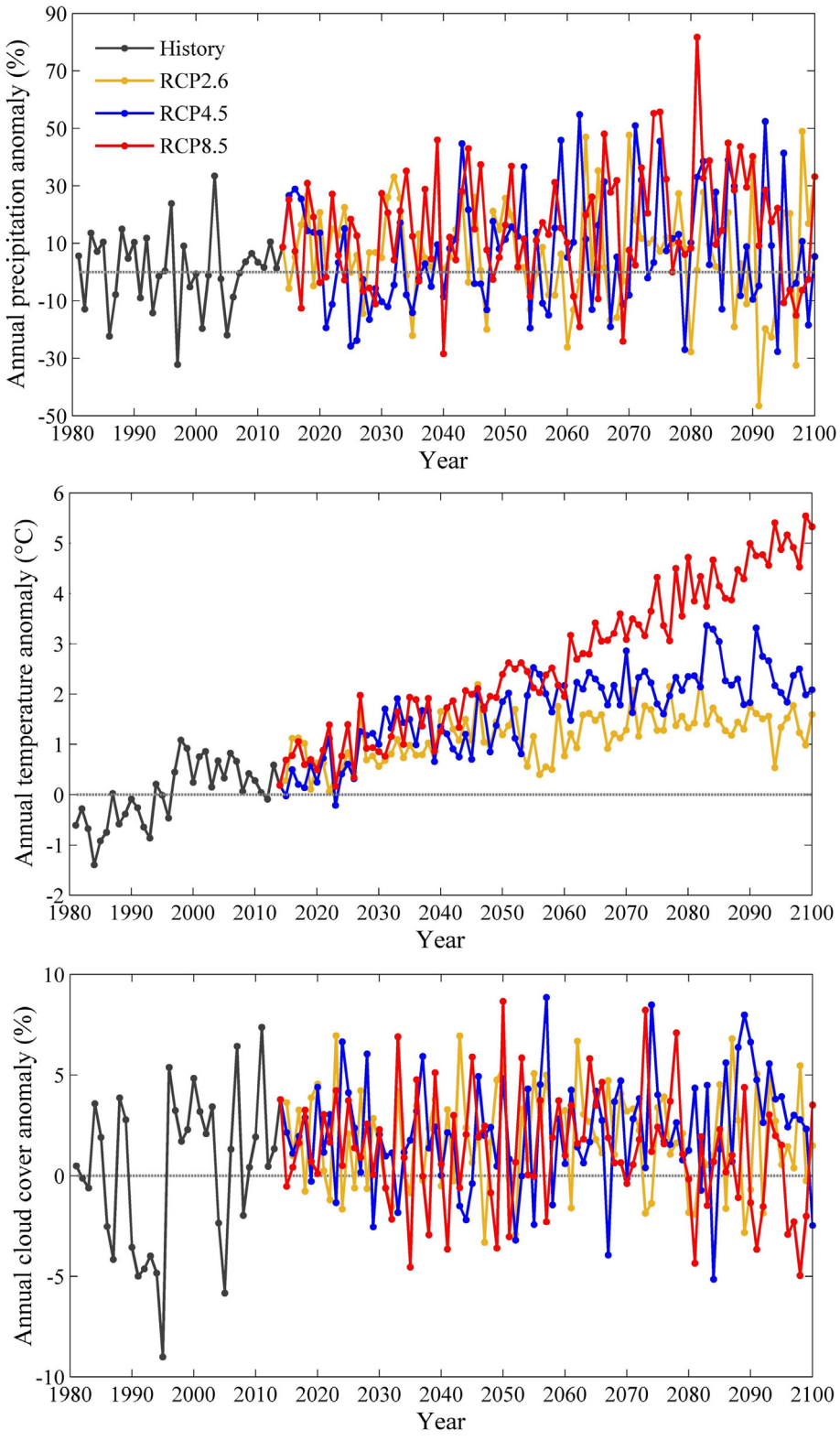

Fig. 2. Annual precipitation, mean temperature, and mean cloud cover anomalies from 1981 to 2100 with the 1981–2010 as the basic period.

2.2. Data description

The observed land use pattern in 2010 with 100-m spatial resolution was generated from Landsat5 TM images, using image preprocessing (geometry correction, image combination, and study region extraction) and image classification. The CLP is classified into six land use types, i.e. farmland, forest, grassland, water bodies, construction land, and unexploited land (Fig. 1). Land type and quality assessment were based on field survey. Around 10% of the field records and photographs from the counties in the CLP were randomly chosen to assess the accuracy of the database. The accuracy of the six classes of land use was >94.3%, which can meet the requirement of mapping accuracy on a 100-m spatial scale (Li et al., 2016). The land use map was spatially resampled to match the spatial

resolution of the PNV distribution based on the maximum percent area of each land use type in the grid.

The simulated land use patterns were derived from the PNV generated by the LPJ-GUESS model. LPJ-GUESS used climate, soil texture, and atmospheric CO_2 concentration as inputs. Climate data, including monthly mean temperature, precipitation, and cloud cover, were from a downscaled dataset with 1-km spatial resolution for 1951–2100, among which the data for the period 1951–2014 were downscaled from the Climate Research Unit Time Series 3.23 dataset with 0.5° spatial resolution (Harris et al., 2014), and the data for 2015–2100 were downscaled from global circulation models (GCM) under RCP scenarios. For the climate change projection, GFDL-ESM2M (Dunne et al., 2012) was used to generate monthly precipitation and NorESM1-M (Bentsen et al., 2013) was used to generate monthly mean temperature (Peng et al., 2018). In addition, the BCC-CSM1.1-M model was used to generate future cloud cover data since it is suitable in reproducing the cloud cover in China (Wu et al., 2014). Soil texture was derived by disaggregating a 0.5° global soil texture dataset (Sitch et al., 2003). Historical CO_2 concentrations for 1951–1958 were obtained from McGuire et al. (2001) and for 1959–2014 from Pieter Tans (National Oceanic and Atmospheric Administration, 2017). CO_2 concentrations for 2015–2100 under RCP scenarios were taken from the RCP Database (RCP Database Comparison, 2009).

2.3. Generating current and future PNV

The LPJ-GUESS model was used to generate the current and future PNV distributions. This model combines the physiological and biophysical processes in the LPJ-DGVM model (Sitch et al., 2003) with tree population dynamics, resource competition, and canopy structure in forest gap models (Bugmann, 2001). As such, it is better for simulating vegetation dynamics at the species or plant function type (PFT) level, which has been widely used in Europe (Hickler et al., 2012), China (Liu et al., 2009; Wang et al., 2016b; Zhao et al., 2014), Africa (Lindeskog et al., 2013), the USA (Snell et al., 2013; Tang et al., 2012), and the global scale (Olin et al., 2015; Smith et al., 2014). The model simulates vegetation dynamics, such as biomass, net primary productivity, leaf area index, and species composition. These vegetation indices can be used to determine the land use patterns based on a certain rule (Hickler et al., 2012; Wolf et al., 2008). In this study, the vegetation classification was based on the biomass from model outputs (Wolf et al., 2008), and the rules can be found in the Supporting Information Table S1.

We parameterized the main tree species and other PFTs to obtain an appropriate representation of vegetation in the study area. Based on the vegetation traits in CLP, the PFTs were determined as boreal needle-leaved evergreen forest (BNE), temperate needle-leaved evergreen forest (TeNE), temperate broadleaved summergreen forest (TeBS), boreal evergreen shrub (BES), temperate summergreen shrub (TSS), and steppe (Table 1). Main model parameters for the PFT were based on those for corresponding or similar PFTs in previous studies (Smith et al., 2014). Some parameters that could be easily measured, such as maximum tree crown area and sapwood and heartwood density, were obtained by our own measurement. In the CLP, we set 8–12 plots with size of 20 × 30 m for each woody PFT. In each plot, the tree crown diameters in eight directions were measured and the crown areas were calculated; then, for each woody PFT, the maximum tree crown areas were determined. Meanwhile, the increment cores of 10–15 trees in each plot were sampled at 1.3 m above the ground with an increment borer and stored in paper straws. In the laboratory, the weight and volume of each increment core were measured and then the woody density for each woody PFT was calculated. The bioclimatic parameters, such as minimum winter temperature for survival and minimum requirement for yearly accumulated temperatures above 5 °C, were derived by spatially overlaying plant species and bioclimatic variables. The corresponding data were obtained from the scientific data center of the Loess Plateau (National Earth System Science Data Sharing Platform, 2015). Detailed parameter information is given in the Supporting Information (see Table S2).

Simulations began with bare ground and no biomass. The model was run for 300 years until the modeled vegetation was in approximate equilibrium with the climate and CO_2 for 1951–1980. Thereafter, the model was run from 1951 to 2100 using the climate and CO_2 datasets described above. In this study, three RCP scenarios, RCP2.6, RCP4.5, and RCP8.5, were used to simulate future PNV distribution.

The simulated PNV distribution should be validated. However, it was difficult to do this with the existing vegetation pattern because of intensive human disturbance. Thus, we generated another PNV distribution using a statistical model, MaxEnt (Phillips et al., 2006), to validate the modeled PNV from LPJ-GUESS. The MaxEnt model can simulate the current PNV pattern based on the existing vegetation pattern and corresponding climate condition. The current PNV distribution generated by the MaxEnt was statistically valid, because the area under the curve of the receiver operating characteristic of each PNV type in the MaxEnt model was >0.81. Besides, the agreement of the current PNV distributions generated from the two models was good. Therefore, the PNV distribution modeled by the LPJ-GUESS in this study is reasonable (see Supporting Information for details).

2.4. Investigating potential land use adjustments

We used the land use patterns derived from the future PNV simulation to investigate the potential adjustments to the existing land use pattern in 2010. We determined the consistency between the observed and potential natural forest and grassland by overlaying observed and simulated land use maps. We also investigated the PNV for the existing farmlands with slopes >25° because they are required to be abandoned by the GGP.

Table 1
Definition of land cover types, PFTs and vegetation types with examples of typical species.

Land cover types	PFTs	Vegetation types	Typical species
Forest	BNE = boreal needle-leaved evergreen forest	Boreal forest	*Picea crassifolia*, *Sabina przewalskii*, *Larix principis-rupprechtii*
	TeNE = temperate needle-leaved evergreen forest	Temperate forest	*Platycladus orientalis* (Linn.) Franco, *Pinus tabuliformis*
	TeBS = temperate broadleaved summergreen forest	Temperate forest	*Quercus wutaishanica* Blume, *Populus davidiana*, *Betula platyphylla*
Shrub	BES = boreal evergreen shrub	Shrubland	*Rhododendron capitatum*, *Rhododendron anthopogonoide*
	TSS = temperate summergreen shrub	Shrubland	*Hippophae rhamnoides* Linn., *Ziziphus jujube*, *Ostryopsis davidiana* Decaisne, *Rosa xanthina* Lindl, *Caragana korshinskii* Kom.
Grass	Steppe (temperate)	Temperate grassland	*Thymus mongolicus*, *Stipa bungeana*, *Sophora davidii*
Barren ground	–	–	Bare ground, rock, snow, ice

3. Results

3.1. Current and future PNV patterns

According to the PNV simulation for 1981–2010, forests account for 29.9% of the CLP, and it was mainly in the southeast region on middle to high elevations (Table 2 and Fig. 3). Specifically, the TeBS, BNE, and TeNE account for 23.1%, 3.8%, and 3.0% of the CLP, respectively. Steppe was mainly in the northwest with 68.1% of the study area. Each of the other vegetation types was <1.5%. Overall, under natural condition, the local land use pattern should be forest in the southeast region and grassland in the northwest region.

With increasing temperature and precipitation projected for 2071–2100, the area and spatial distribution of each vegetation type changed in the PNV simulation (Fig. 3 and Table 2). Specifically, potential forested areas would decrease from 29.9% in 1981–2010 to 7.9%–23.8% in 2071–2100, and potential steppe areas would increase from 68.1% to 74.3%–90.5% (Table 2). This change in area was due to vegetation type conversion from forest to steppe (Table 3). Overall, the areas with vegetation type conversion accounted for 27.6%, 29.4%, and 31.7% of CLP under RCP2.6, RCP4.5, and RCP8.5, respectively. The areas with changes in vegetation types were mainly in the southeastern and western parts of the study area (see Supporting Information Fig. S1). Over 40% of each forest type was projected to be converted to steppe. The magnitude of vegetation type conversion decreased with increasing intensity of radiative forcing (Table 3).

3.2. Differences between observed and simulated land use patterns

The land use map in 2010 was overlaid with the simulated maps for 2071–2100 to investigate the differences between the observed and simulated future land use patterns. As only forest and grassland are the common vegetation types in the two datasets, their areas and spatial distributions were compared. Approximately 25.3%, 42.1%, and 55.0% of the observed forests in 2010 were projected to remain during 2071–2100 under RCP2.6, RCP4.5, and RCP8.5, respectively. The rest of the existing forested area was expected to be more suitable for steppe, and these regions were mainly in the center and northern parts of CLP (Fig. 4). Approximately 91.9%, 87.0%, and 79.3% of the existing grassland in 2010 were projected to remain during 2071–2100 under RCP2.6, RCP4.5, and RCP8.5, respectively. The rest of the existing grassland was expected to be more suitable for forests, which were mostly in the southern and western parts of CLP (Fig. 5).

In addition, we overlaid the existing steep farmland in 2010 with the averaged PNV from 2071 to 2100 to investigate potential of GGP in future (Fig. 6). In general, grassland rather than forest was preferred for the steep farmland (see Supporting Information Table S3). Specifically, grassland accounted for 60.9–84.8% of the existing steep farmland, mainly in the central and western parts of CLP, while the corresponding values for forest was 14.7–36.8% in the central and southern parts of CLP. In addition, the percent area of grassland decreased while the area of forestland increased with the increasing intensity of radiative forcing.

Table 2
Percent area (%) for each PFT during current and future time periods.

PFTs	1981–2010	2071–2100		
		RCP2.6	RCP4.5	RCP8.5
BNE	3.8	2.0	2.3	2.5
TeNE	3.0	2.2	7.6	14.4
TeBS	23.1	3.7	4.3	6.9
BES	0.5	0.7	0.7	0.4
TSS	0.8	0.6	1.8	1.5
Steppe	68.1	90.5	83.1	74.3
No vegetation	0.7	0.3	0.2	0

4. Discussion

4.1. Vegetation response to climate change

Although climate dominates the spatiotemporal characteristics of vegetation, precipitation and temperature may have different impacts (Wu et al., 2015). Sun et al. (2015) studied this issue for CLP. Precipitation was found to be positively correlated with NDVI over most regions. However, temperature and NDVI were negatively correlated in the northwest, and they were positively correlated in the center and southeast. The positive relationship between precipitation and NDVI implies that precipitation is the limiting factor for vegetation; however, higher temperatures promote vegetation growth in areas with less water stress, such as the southwest part of CLP.

If the effects of precipitation and temperature on vegetation are invariant over time, the increased precipitation and temperature projected for 2071–2100 (Peng et al., 2018) could further improve vegetation and support more forests. However, it appears that the PNV would not change as expected since a large proportion of forests would be converted to steppe (Table 3), which is similar to vegetation projections for Europe (Hickler et al., 2012; Wolf et al., 2008). The conversion from forest to steppe would possibly be caused by the combined effects of precipitation and temperature. The increased temperature is expected to increase potential evapotranspiration (ET_0) by 12.7–23.9% under different RCPs during 2071–2100 (Peng et al., 2017). As the actual evapotranspiration (ET_a) is proportional to ET_0, ET_a would likely increase with a similar magnitude to ET_0. However, the corresponding increase in precipitation is projected to be 6–22% (Peng et al., 2018), which is a smaller increase than ET_0. More evapotranspiration and less precipitation would result in less available water resources for CLP at the end of this century. Therefore, it is likely that greater water stress would decrease the forested areas.

In this study, the type of forest conversion found for CLP differed from other regions. Specifically, the main forest conversion would be from temperate broadleaved forest to temperate conifer forest (Table 3). Research in Europe found a future forest conversion from boreal conifer forest to temperate broadleaved forest (Hickler et al., 2012; Koca et al., 2006). CLP's temperate and boreal forests are located in mid-latitudes, and the European temperate and boreal forests are at significantly higher latitudes (Hickler et al., 2012; Koca et al., 2006). Subsequently, the impacts of climate change on different forest types vary spatially. Similar to the projected decrease in forested area and the increase in steppe, the conversion from temperate broadleaved to conifer forests on CLP would likely be caused by decreased available water resources; temperate conifer forests can better adapt to a dry climate than broadleaved forests (Gilliam, 2016).

With a changing climate, the PNV types would shift in large areas in CLP, the USA (Tang et al., 2012), and Europe (Hickler et al., 2012; Koca et al., 2006; Wolf et al., 2008). The changes in vegetation type vary between regions because of spatial heterogeneity; further, the increasing temperature and precipitation does not mean more forests due to their combined effects. Therefore, qualitative interpretation of the impacts of climate change on vegetation should be done with caution, especially on large spatial scales.

4.2. Adjusting human-influenced land use patterns

Most of the previous studies focused on projection of the PNV patterns and investigated the responses of the PNV to future climate change (Hickler et al., 2012; Koca et al., 2006; Tang et al., 2012; Wolf et al., 2008). However, the current study extended these to guide land management by comparing the projected vegetation pattern with the current observation. The research approach and results in this study are very important for land management, especially for the revegetated region, which can provide operable plans to adjust unreasonable land use patterns.

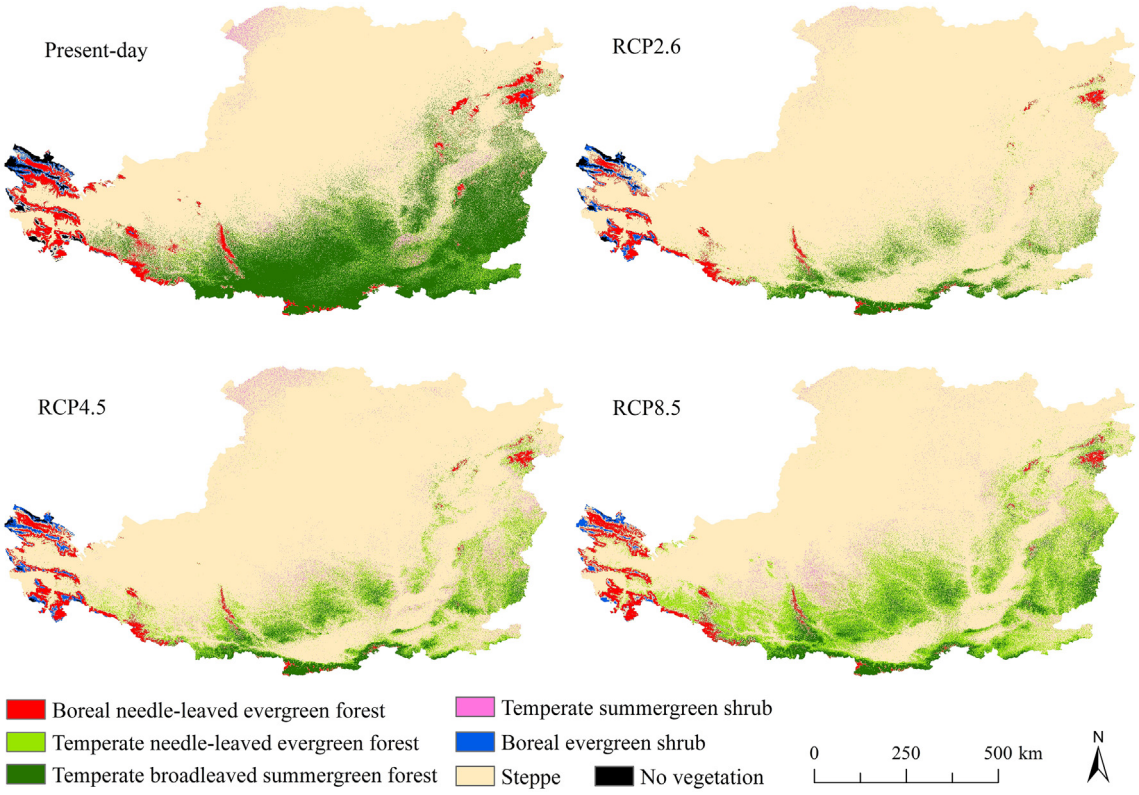

Fig. 3. Modeled current (averaged for 1981–2010) and future (averaged for 2071–2010) PNV distributions.

As climate change strongly influences vegetation, it is important to incorporate knowledge of PNV and climate change adaptation into revegetation programs (Breed et al., 2013). According to the PNV from 2071 to 2100, 25.3–55.0% of the observed forests and 79.3–91.9% of the observed grassland in 2010 were projected to remain (Figs. 4 and 5). The projected change in the existing land use pattern from 2071 to 2100 suggests the urgency of climate change adaptation. Climate change adaptation strategies can be viewed as a risk management component of the revegetation (Dai et al., 2016). Previous studies have developed numerous adaptive strategies and actions to adapt and mitigate climate change, such as planning and implementing strategies at a local scale, enabling vegetation to respond to change, buffering protected areas, and promoting spontaneous recovery (Bolte et al., 2009; Galatowitsch et al., 2009; Millar et al., 2007). For CLP, and even the whole of China, research on adaptation to future climate change for the revegetation is insufficient.

More research should investigate adaptive measures. Firstly, according to our results, the existing forest/grass pattern could be adjusted to better cope with future climate change (Figs. 4 and 5). Secondly, vegetation restoration policies should be revised to consider future climatic adaptation at the local scale, not just the topographical factors (Fig. 6). Thirdly, requiring a lot of computation power, this study only selected the CLP as study region; however, it should be extended to the whole China to provide more valuable information for China's eco-environmental construction.

4.3. Uncertainty analysis

The climatic data used to drive the LPJ-GUESS model could have introduced uncertainties into our study. The climate data for the current period were from observations, so they were accurate and reliable. However, the data for the future period were downscaled from GCMs. GCM-projected climate data can differ between the models because of differing model structures, initial boundary conditions, and emission scenarios (Hawkins and Sutton, 2009). For example, Xu and Xu (2012) evaluated the ability of GCMs to simulate China's climate and found that GCMs effectively reflected the warming tendency, but the precipitation predictions were limited. The uncertainty from climatic data can be reduced to some extent either by using the ensemble mean or by choosing the best model. In this study, based on the evaluation of 28 GCMs in our previous study (Peng et al., 2018), we used the GCMs with better performance in hindcasting the observed historical climates. Further, our downscaling procedure has been validated in detail. Therefore, our procedure for generating climate change scenarios

Table 3
Ratio (%) of type shift from current time period (1981–2010) to the end of the century (2071–2100) under three RCP scenarios.

	RCP2.6							RCP4.5							RCP8.5						
	BNE	TeNE	TeBS	BES	TSS	Steppe	NoV	BNE	TeNE	TeBS	BES	TSS	Steppe	NoV	BNE	TeNE	TeBS	BES	TSS	Steppe	NoV
BNE	42.5	1.4	1.8	0	0	54.3	0	44.8	4.7	3.5	0	0.1	46.9	0	43.8	8.7	6.9	0	0.2	40.4	0
TeNE	0	2.1	1.5	0	0.8	95.6	0	0	10.4	1.5	0	4.1	84	0	0	28.1	5	0	2	64.9	0
TeBS	0.1	7.6	14.5	0	0.9	76.9	0	0.1	24	15.6	0	3	57.3	0	0	36.7	22.5	0	1.1	39.7	0
BES	16.7	0	0	39.8	0	43.5	0	32.8	0	0	19.4	0	47.8	0	51.7	0	0	0.3	0	48	0
TSS	0	0.5	0.1	0	2.5	96.9	0	0	1.2	0.1	0	7.1	91.6	0	0	5.2	0.6	0	4.2	90	0
Steppe	0.4	0.5	0.4	0.2	0.5	98	0	0.6	2.3	0.7	0.1	1.4	94.9	0	0.7	6.9	1.9	0	1.6	88.9	0
NoV	0	0	0	47	0	0.4	52.6	0.4	0	0	72.4	0	4.7	22.5	3.8	0	0	55.2	0	39	2

Note: NoV represents no vegetation.

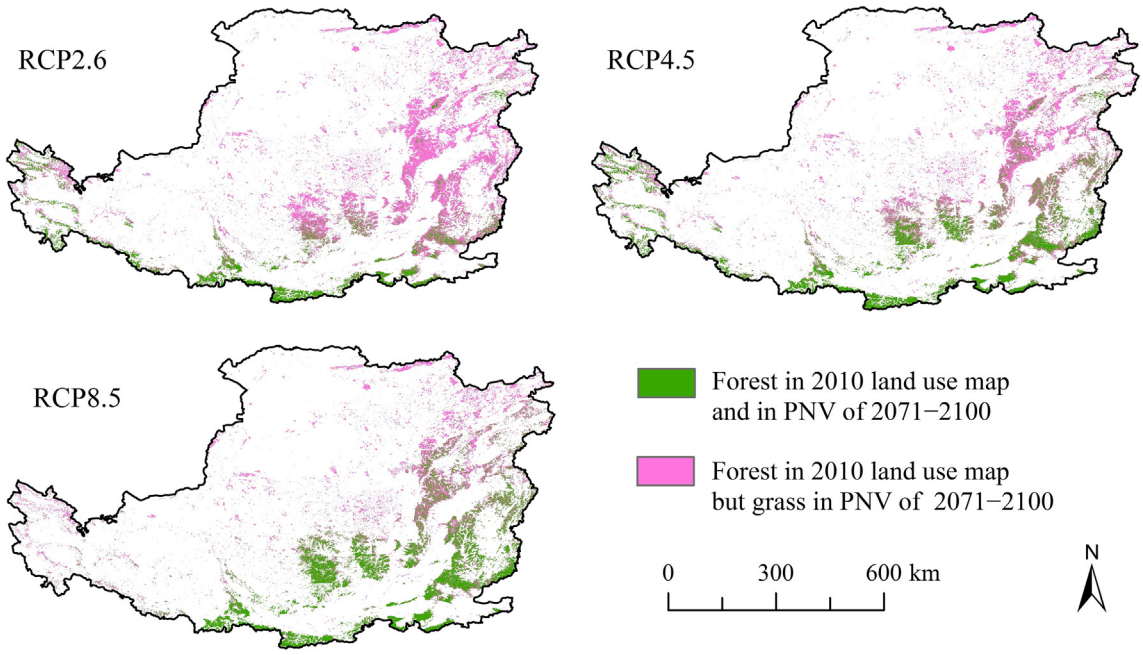

Fig. 4. Spatial overlay between forest pattern in 2010 and the PNV distribution at the end of the century (averaged for 2071–2100) under three RCP scenarios.

can reduce the uncertainty from GCMs; however, other methods, such as the ensemble mean, could be used in future work.

The other uncertainty was from the data transformation. To compare the modeled and observed land use patterns, we transformed the biomass to the land use types listed in Supporting Information Table S1. Although this procedure has been proven to be reliable in other studies (Hickler et al., 2006; Hickler et al., 2012; Wolf et al., 2008), the veracity of the PNV distribution may have been affected by the slight change in the classification system. As our evaluation of the PNV distribution showed that the model had satisfactory performance, we did not explore this source of uncertainty in detail. We conducted a simulation at a 1-km resolution, which is the highest spatial resolution used to date at such a large spatial scale; however, this resolution still cannot match the spatial scale of 100 m land use map. To match the spatial resolution of the two datasets, we resampled the land use map to the coarse resolution of the LPJ-GUESS model. This process may have introduced some uncertainties in calculating the areas of different land use types. Thus, although our current 1 km resolution is higher than most other studies, an even higher resolution of <1 km data should be employed. However, each land use type in the CLP had good regionalization (Li et al., 2016), and this issue likely had little impact on our results.

5. Conclusions

To adapt to future climate change, appropriate land use patterns are desired. In this study, we chose CLP, a typical revegetation region, to generate the PNV for the period 2071–2100 and further discussed the

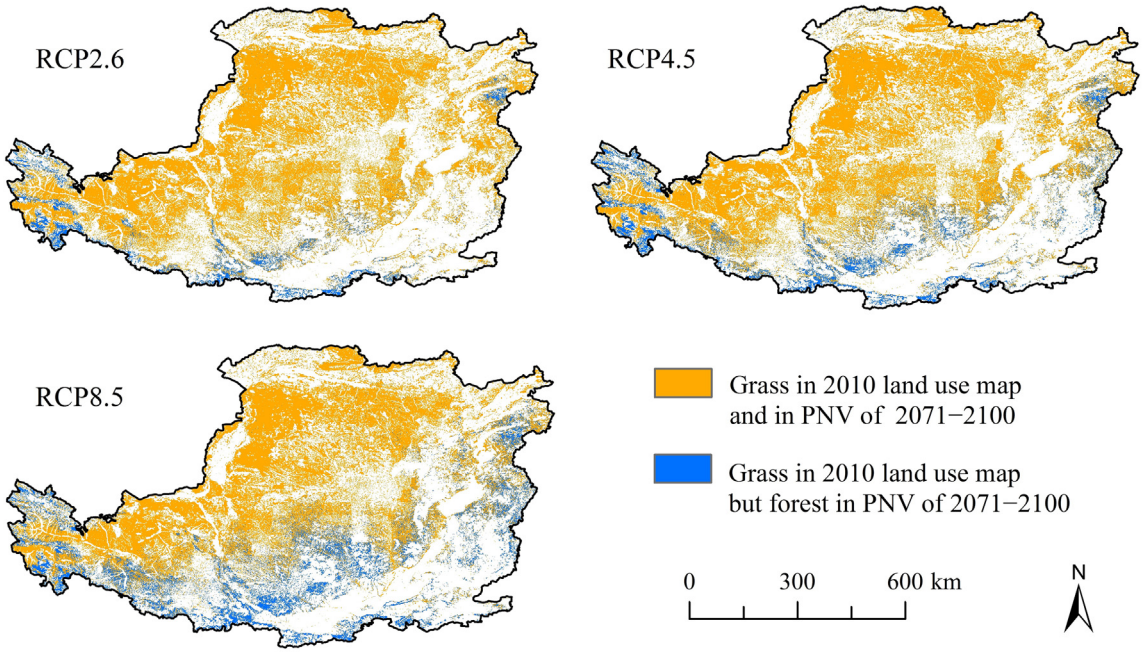

Fig. 5. Spatial overlay between grassland pattern in 2010 and the PNV distribution at the end of the century (averaged for 2071–2100) under three RCP scenarios.

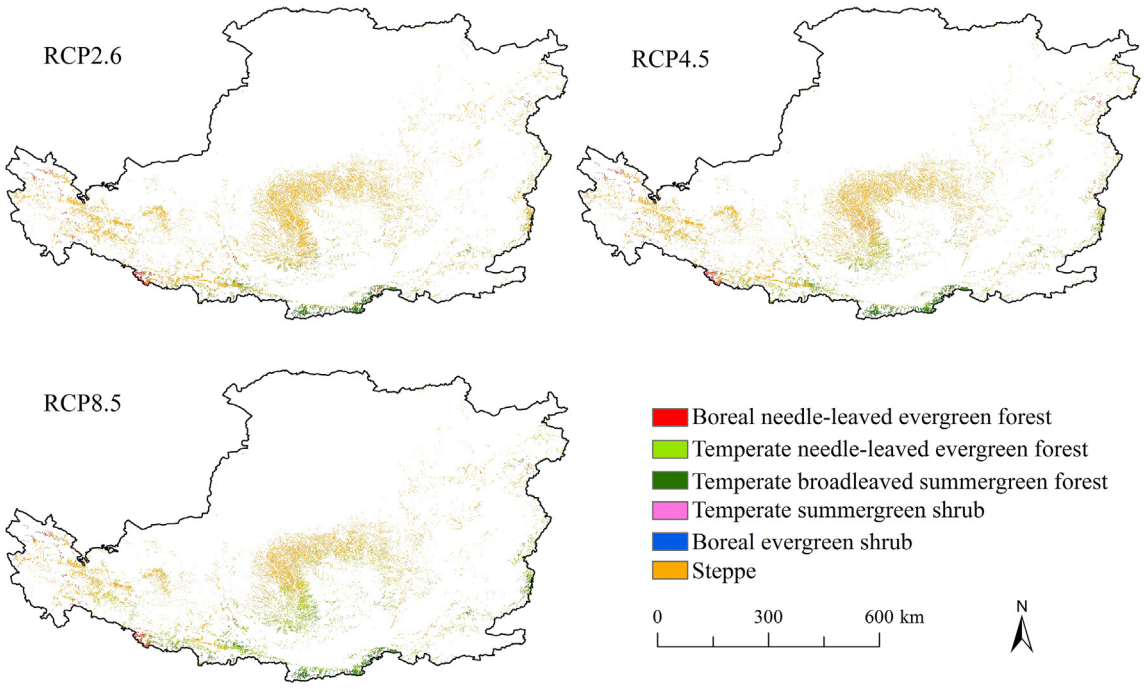

Fig. 6. Spatial overlay between steep farmland distribution in 2010 and the PNV distribution under future (averaged for 2071–2100) climate condition.

potential adjustment in the existing land use pattern. Compared with 1981–2010, the projected PNV over 2071–2100 would have less forest and more steppe because of drier climate. Subsequently, 25.3–55.0% of the observed forests and 79.3–91.9% of the observed grasslands in 2010 can be kept over 2071–2100, and the rest of the existing forested area and grassland were expected to be more suitable for steppes and forests, respectively. To meet the request of China's Grain for Green Project, 60.9–84.8% of the existing steep farmland could be converted to grassland and the other for forest. Our results highlight the importance in adjusting the existing vegetation pattern to adapt to climate change. The research approach is extendable and provides a framework to evaluate the sustainability of the existing land use pattern under future climate.

Acknowledgements

This study is jointly supported by National Natural Science Foundation of China (41601058 & 41761144060) and CAS Light of West China Program (XAB2015B07). The authors thank the HPC of Northwest A&F University, which provides the high-performance computers for us to run the LPJ-GUESS model.

Appendix A. Supplementary data

Supplementary data to this article can be found online at https://doi.org/10.1016/j.scitotenv.2018.05.194.

References

Albani, M., Medvigy, D., Hurtt, G.C., Moorcroft, P.R., 2006. The contributions of land-use change, CO_2 fertilization, and climate variability to the Eastern US carbon sink. Glob. Chang. Biol. 12, 2370–2390.

Bentsen, M., Bethke, I., Debernard, J.B., Iversen, T., Kirkevåg, A., Seland, Ø., et al., 2013. The Norwegian Earth System Model, NorESM1-M — part 1: description and basic evaluation of the physical climate. Geosci. Model Dev. 6, 687–720.

Bolte, A., Ammer, C., Löf, M., Madsen, P., Nabuurs, G.-J., Schall, P., et al., 2009. Adaptive forest management in central Europe: climate change impacts, strategies and integrative concept. Scand. J. For. Res. 24, 473–482.

Breed, M.F., Stead, M.G., Ottewell, K.M., Gardner, M.G., Lowe, A.J., 2013. Which provenance and where? Seed sourcing strategies for revegetation in a changing environment. Conserv. Genet. 14, 1–10.

Bugmann, H., 2001. A review of forest gap models. Clim. Chang. 51, 259–305.

Chen, Y., Wang, K., Lin, Y., Shi, W., Song, Y., He, X., 2015. Balancing green and grain trade. Nat. Geosci. 8, 739–741.

Chiarucci, A., Araújo, M.B., Decocq, G., Beierkuhnlein, C., Fernández-Palacios, J.M., 2010. The concept of potential natural vegetation: an epitaph? J. Veg. Sci. 21, 1172–1178.

Chinese National Ecosystem Research Network, 2017. Meteorological Data. www.cnern.org.cn (accessed 26 Novermber 2017).

Crouzeilles, R., Curran, M., Ferreira, M.S., Lindenmayer, D.B., Grelle, C.E.V., Rey Benayas, J.M., 2016. A global meta-analysis on the ecological drivers of forest restoration success. Nat. Commun. 7, 11666.

Dai, E., Wu, Z., Ge, Q., Xi, W., Wang, X., 2016. Predicting the responses of forest distribution and aboveground biomass to climate change under RCP scenarios in southern China. Glob. Chang. Biol. 22, 3642–3661.

Deng, L., Liu, G., Shangguan, Z., 2014. Land-use conversion and changing soil carbon stocks in China's 'Grain-for-Green' Program: a synthesis. Glob. Chang. Biol. 20, 3544–3556.

Dunne, J.P., John, J.G., Adcroft, A.J., Griffies, S.M., Hallberg, R.W., Shevliakova, E., et al., 2012. GFDL's ESM2 global coupled climate–carbon earth system models. Part I: physical formulation and baseline simulation characteristics. J. Clim. 25, 6646–6665.

Feng, X., Fu, B., Piao, S., Wang, S., Ciais, P., Zeng, Z., et al., 2016. Revegetation in China's Loess Plateau is approaching sustainable water resource limits. Nat. Clim. Chang. 6, 1019–1022.

Friend, A.D., Lucht, W., Rademacher, T.T., Keribin, R., Betts, R., Cadule, P., et al., 2014. Carbon residence time dominates uncertainty in terrestrial vegetation responses to future climate and atmospheric CO_2. Proc. Natl. Acad. Sci. 111, 3280–3285.

Galatowitsch, S., Frelich, L., Phillips-Mao, L., 2009. Regional climate change adaptation strategies for biodiversity conservation in a midcontinental region of North America. Biol. Conserv. 142, 2012–2022.

Gilliam, F.S., 2016. Forest ecosystems of temperate climatic regions: from ancient use to climate change. New Phytol. 212, 871–887.

Harris, I., Jones, P., Osborn, T., Lister, D., 2014. Updated high-resolution grids of monthly climatic observations—the CRU TS3.10 Dataset. Int. J. Climatol. 34, 623–642.

Hawkins, E., Sutton, R., 2009. The potential to narrow uncertainty in regional climate predictions. Bull. Am. Meteorol. Soc. 90, 1095–1107.

Hickler, T., Prentice, I.C., Smith, B., Sykes, M.T., Zaehle, S., 2006. Implementing plant hydraulic architecture within the LPJ Dynamic Global Vegetation Model. Glob. Ecol. Biogeogr. 15, 567–577.

Hickler, T., Vohland, K., Feehan, J., Miller, P.A., Smith, B., Costa, L., et al., 2012. Projecting the future distribution of European potential natural vegetation zones with a generalized, tree species-based dynamic vegetation model. Glob. Ecol. Biogeogr. 21, 50–63.

Koca, D., Smith, B., Sykes, M.T., 2006. Modelling regional climate change effects on potential natural ecosystems in Sweden. Clim. Chang. 78, 381–406.

Li, J., Li, Z., Lü, Z., 2016. Analysis of spatiotemporal variations in land use on the Loess Plateau of China during 1986–2010. Environ. Earth Sci. 75, 997.

Li, J., Peng, S., Li, Z., 2017. Detecting and attributing vegetation changes on China's Loess Plateau. Agric. For. Meteorol. 247, 260–270.

Lindeskog, M., Arneth, A., Bondeau, A., Waha, K., Seaquist, J., Olin, S., et al., 2013. Implications of accounting for land use in simulations of ecosystem carbon cycling in Africa. Earth Syst. Dynam. 4, 385–407.

Liu, R., Li, N., Su, H., Sang, W., 2009. Simulation and analysis on future carbon balance of three deciduous forests in Beijing mountain area,warm temperate zone of China. Chin. J. Plant Ecol. 33, 516–534 (in Chinese).

McGuire, A.D., Sitch, S., Clein, J.S., Dargaville, R., Esser, G., Foley, J., et al., 2001. Carbon balance of the terrestrial biosphere in the Twentieth Century: analyses of CO_2, climate and land use effects with four process-based ecosystem models. Glob. Biogeochem. Cycles 15, 183–206.
Millar, C.I., Stephenson, N.L., Stephens, S.L., 2007. Climate change and forests of the future: managing in the face of uncertainty. Ecol. Appl. 17, 2145–2151.
National Earth System Science Data Sharing Platform, 2015. The Scientific Data Center of the Loess Plateau. http://loess.data.ac.cn (accessed 25 Novermber 2017).
National Oceanic and Atmospheric Administration, 2017. Trends in Atmospheric Carbon Dioxide. http://www.bonnchallenge.org/content/challenge (accessed 26 November 2017).
Olin, S., Lindeskog, M., Pugh, T.A.M., Schurgers, G., Wårlind, D., Mishurov, M., et al., 2015. Soil carbon management in large-scale Earth system modelling: implications for crop yields and nitrogen leaching. Earth Syst. Dynam. 6, 745–768.
Peng, S., Ding, Y., Wen, Z., Chen, Y., Cao, Y., Ren, J., 2017. Spatiotemporal change and trend analysis of potential evapotranspiration over the Loess Plateau of China during 2011–2100. Agric. For. Meteorol. 233, 183–194.
Peng, S., Gang, C., Cao, Y., Chen, Y., 2018. Assessment of climate change trends over the Loess Plateau in China from 1901 to 2100. Int. J. Climatol. 38, 2250–2264.
Phillips, S.J., Anderson, R.P., Schapire, R.E., 2006. Maximum entropy modeling of species geographic distributions. Ecol. Model. 190, 231–259.
Piao, S., Friedlingstein, P., Ciais, P., Zhou, L., Chen, A., 2006. Effect of climate and CO_2 changes on the greening of the Northern Hemisphere over the past two decades. Geophys. Res. Lett. 33, L23402.
Piao, S., Sitch, S., Ciais, P., Friedlingstein, P., Peylin, P., Wang, X., et al., 2013. Evaluation of terrestrial carbon cycle models for their response to climate variability and to CO_2 trends. Glob. Chang. Biol. 19, 2117–2132.
Pielke, R.A., 2005. Land use and climate change. Science 310, 1625–1626.
RCP Database Comparison, 2009. RCP Database (Version 2.0). http://www.iiasa.ac.at/web-apps/tnt/RcpDb (accessed 20 Novermber 2017).
Sitch, S., Smith, B., Prentice, I.C., Arneth, A., Bondeau, A., Cramer, W., et al., 2003. Evaluation of ecosystem dynamics, plant geography and terrestrial carbon cycling in the LPJ dynamic global vegetation model. Glob. Chang. Biol. 9, 161–185.
Smith, B., Prentice, I.C., Sykes, M.T., 2001. Representation of vegetation dynamics in the modelling of terrestrial ecosystems: comparing two contrasting approaches within European climate space. Glob. Ecol. Biogeogr. 10, 621–637.
Smith, B., Wårlind, D., Arneth, A., Hickler, T., Leadley, P., Siltberg, J., et al., 2014. Implications of incorporating N cycling and N limitations on primary production in an individual-based dynamic vegetation model. Biogeosciences 11, 2027–2054.
Snell, R.S., Cowling, S.A., Smith, B., 2013. Simulating regional vegetation-climate dynamics for Middle America: tropical versus temperate applications. Biotropica 45, 567–577.
Sun, W., Song, X., Mu, X., Gao, P., Wang, F., Zhao, G., 2015. Spatiotemporal vegetation cover variations associated with climate change and ecological restoration in the Loess Plateau. Agric. For. Meteorol. 209, 87–99.
Tang, G., Beckage, B., Smith, B., 2012. The potential transient dynamics of forests in New England under historical and projected future climate change. Clim. Chang. 114, 357–377.
Verdone, M., Seidl, A., 2017. Time, space, place, and the Bonn Challenge global forest restoration target. Restor. Ecol. 25, 903–911.
Wang, S., Fu, B., Piao, S., Lü, Y., Ciais, P., Feng, X., et al., 2016a. Reduced sediment transport in the Yellow River due to anthropogenic changes. Nat. Geosci. 9, 38–41.
Wang, W., Rinke, A., Moore, J.C., Cui, X., Ji, D., Li, Q., et al., 2016b. Diagnostic and model dependent uncertainty of simulated Tibetan permafrost area. Cryosphere 10, 287–306.
Wolf, A., Callaghan, T.V., Larson, K., 2008. Future changes in vegetation and ecosystem function of the Barents Region. Clim. Chang. 87, 51–73.
Wu, T., Song, L., Li, W., Wang, Z., Zhang, H., Xin, X., et al., 2014. An overview of BCC climate system model development and application for climate change studies. J. Meteorol. Res. 28, 34–56.
Wu, D., Zhao, X., Liang, S., Zhou, T., Huang, K., Tang, B., et al., 2015. Time-lag effects of global vegetation responses to climate change. Glob. Chang. Biol. 21, 3520–3531.
Xu, C., Xu, Y., 2012. The projection of temperature and precipitation over China under RCP scenarios using a CMIP5 multi-model ensemble. Atmos. Ocean. Sci. Lett. 5, 527–533.
Zerbe, S., 1998. Potential natural vegetation: validity and applicability in landscape planning and nature conservation. Appl. Veg. Sci. 1, 165–172.
Zhao, G., Mu, X., Wen, Z., Wang, F., Gao, P., 2013. Soil erosion, conservation, and eco-environment changes in the loess plateau of China. Land Degrad. Dev. 24, 499–510.
Zhao, M., Yue, T., Zhao, N., Sun, X., Zhang, X., 2014. Combining LPJ-GUESS and HASM to simulate the spatial distribution of forest vegetation carbon stock in China. J. Geogr. Sci. 24, 249–268.